449

Simulation the Behavior of Passive Rigid Pile in Sandy Soil

Mahdi O. Karkush [*] **& Ghofran S. Jaffar**

Department of Civil Engineering, University of Baghdad, Baghdad, Iraq
[*]E-mail: mahdi_karkush@coeng.uobaghdad.edu.iq

Highlights:

- This work investigated the effects of constructing a new foundation nearby an existing pile foundation.
- The new foundation applies stresses to the soil and these stresses will be transferred through the soil to the adjacent pile foundation.
- The existing pile foundation, loaded and unloaded, was assumed rigid and located at varied distances from the new foundation.

Abstract. This research studied the behavior of a rigid pile driven into sandy soil and subjected to soil movement. The behavior of the pile was simulated in two cases: loaded and unloaded. The modeled piles were made of aluminum and had a diameter (D) of 10 mm. Embankment loads were applied at three different distances from the face of the pile (2.5, 5, and 10) D. Strain gauges were fixed at four points along the pile shaft using a half-bridge configuration to measure the strains resulted from the lateral movement of the soil. The results obtained from the physical model were the lateral and vertical movements at the surface of the soil and the bending strain along the pile shaft. These results were analyzed numerically to calculate the bending moment, pile rotation, pile deflection, shear force, and soil reaction profiles. Some of these results were measured experimentally and others were calculated theoretically based on the measured strains. The maximum deflection of the axially loaded pile was more than that in the unloaded pile by 26%, 108%, and 159%, with the embankment at distances (2.5, 5, and 10) D, respectively. The rigid pile provided more resistance to the pressure generated from the soil movement.

Keywords: *embankment; numerical simulation; passive; pile; rigid; sandy soil.*

1   Introduction

In the case of lateral loads, direct or passive, piles behave like transversely loaded beams and transfer loads to the soil. When lateral loading is applied to the piles, a part or whole of the pile tries to move horizontally in the loading direction, which causes bending moment, rotation, and movement of the pile [1,2]. A laterally loaded pile may be classified as passive or active depending on the way of transferring the load to the piles [3,4]. Active piles are principally loaded at their head and the lateral load is transferred to the soil; examples are piles used in

foundations of transmission towers and offshore structures. Passive piles usually sustain lateral thrusts along their embedded depth, coming from the rearrangement and movement of soil particles surrounding them, such as piles in a moving slope [5]. Soil movement, in practice, is encountered when the piles are placed near to a deep excavation, tunneling, unstable slopes, landslides, unstable riverbanks with a highly fluctuating water level and bridge abutments [6]. Piles supporting the abutments of a bridge may be influenced by a combination of loads, lateral load generated from soil movement and axial load [7]. Generally, little information is available about the performance of piles supporting a combination of vertical load and soil movement simultaneously [8].

The influence of 3D soil deformation on the performance of laterally loaded piles driven in sandy soil was investigated by conducting a series of model tests. The 3D deformation of the soil surface around the piles was obtained by Stereo-PIV. The results of the experimental work proved that passive piles restrain the lateral soil movement when the spacing between the piles is less than 6 B. Also, passive piles will affect the response of the active pile when the spacing is less than 4 B [9]. A simple analytical method was used for simulating the effects of soil movement resulted from soil excavation on the behavior of pile groups. The finite difference method with the Winkler model was used for modeling the pile-soil interaction in multi-layered soil. The response of the pile group obtained from the proposed method was in good agreement with the results obtained from centrifuge model tests [9-11]. Ti, *et al*. [12] reviewed the available literature describing the behavior of passive piles in different types of soils. The behavior of passive piles can be summarized by referring to four aspects: the effects of horizontal soil movement on the piles, the embankment supported by the piles, the slope stabilized by the piles, and the effects of excavation on nearby piles.

The behavior of piles at the edge of an embankment, subjected to passive loads from an adjacent embankment was modeled by using a combination of 2D and 3D analytical solutions. The results of the analytical solutions were in good agreement with those measured in the field [13]. A new shear box was developed to measure the effect of lateral soil movement on the bending moment of vertical piles. Two tests conducted on instrumented piles of two deferent diameters are presented. The test results indicate that the limiting force mobilized along the piles in movable soil is quite similar to that due to lateral loads. Ersoy and Yildirim [14] investigated the behavior of piles subjected to lateral movement of soil resulted from slopes by using a large-scale shear box. The results of the tests were compared with those found in the literature to contribute to the understanding of the behavior of passive piles. The effects of lowering the groundwater table resulted from the consolidation of the soil on the passive shaft resistance (PSR) of an existing pile were investigated by using an analytical approach and a finite element approach to calculate the variation of soil pressure

along the shaft of the pile. It was found that the depth of the dewatered zone has a significant effect on the magnitude of the induced PSR [15].

Karkush and Kareem [16,17] have studied the performance of passive piles in fine-grained textured soil contaminated with two ratios of petroleum products (MFO) under the effects of lateral soil movement. The test results showed that increasing the content of contaminants in the soil increased the impacts of the embankment on the response of the passive piles. Ren, *et al.* [18] conducted large centrifuge model tests of two design schemes to simulate sheet-pile wharves with a load-relief platform in homogeneous fine sand to get the distribution of lateral soil pressure on a pile, distinguishing between the passive and active parts of the pile. The present study investigated the influence of the lateral movement of soil resulted from a nearby embankment on the performance of a single rigid pile embedded in sandy soil. The performance of a passive pile was investigated by measuring the vertical and lateral displacement of the pile at the surface of the soil and the strains generated along the shaft of the pile. The measured strains were used to calculate the bending moment, deflection, rotation, shear force, and soil reaction exerted on the model pile.

2 Soil Sampling and Used Materials

2.1 Soil Sampling and Model Pile Properties

The soil sample used in the tests was classified as river sand (SP-SM) according to the unified soil classification system (USCS). The properties of the soil samples were measured according to the ASTM and BS specifications [19,20]. The geotechnical properties of the soil sample are listed in Table 1.

Table 1   Properties of soil sample and model pile.

Property	Value	Property	Value
Gs	2.67	φ (°) at Dr = 56%	35°
Cu	2.934	c (kPa)	9
Cc	1.188	E_{oed} (kPa)	65770
Fines (%)	9.8	Outer diameter of pile (D)	10 mm
Sand (%)	90.2	Wall thickness of pile	1 mm
Dr (%)	56	Length of pile (L)	500 mm
γ_{dmin} (kN/m^3)	11.87	Weight of pile	42 gm
γ_{dmax} (kN/m^3)	15.14	Density of pile material	2.97 gm/cm^3
γ_d (kN/m^3) at Dr = 56%	13.5	Modulus of elasticity (Ep)	69.871 GPa

Aluminum closed-end pipe piles were used as model piles in the experimental physical model. The piles had a circular cross-sectional area and a total length of 500 mm. The engineering properties of the model pile material are given in Table 1. The ratio of (L/D) of all model piles was equal to 50 and the embedded depth

of the piles used in this study was 360 mm, where the model piles behaved as rigid piles according to the flexibility factor (K_R) [21].

A half-bridge pattern of four pairs of strain gauges were fixed on the model piles to measure the bending strain. On the two vertical lines of the front and rear sides with respect to the surcharge location, four pairs of strain gauges were installed on the outer surface of the tested piles with a spacing of 120 mm, as shown in Figure 1. To protect the strain gauges from damage during the insertion of the piles, the strain gauges were sealed with 1 mm epoxy resin. The connection wires of the strain gauges were wrapped and fixed to the outer surface of the piles using glue and tape.
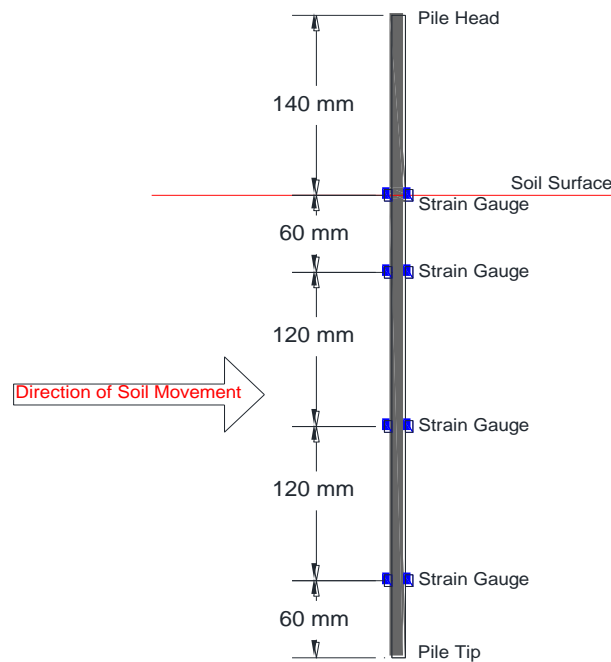

Figure 1 Locations of strain gauges on the model pile.

2.2   Physical Modeling of the Problem

The physical model was a steel container of dimensions (800×800×800 mm). A loading frame was used for inserting the piles into the soil and was also used for applying the surcharge load. The frame consisted of two beams with a U-section in the horizontal direction to allow the hydraulic jack to move horizontally along the beams and two columns in the vertical direction with a square section. At the sides of the columns, holes were made to help in controlling the height and verticality of the loading frame. The maximum capacity of the hydraulic jack was

about 10 tons according to its catalog. The load cell was attached to a cylindrical steel shaft, which was used as an extension. The raining technique was used to pour soil freely into the container by using a cone. When the sand rose in the container to a certain thickness, the cone was raised with a distance equal to the sand thickness that developed in the container to maintain the required distance for falling to achieve the desired density. The sand was poured from several heights of (100, 200, 300, and 400) mm to get the relation between the height of the pouring and the density of the soil. The bedding soil was prepared with a dry unit weight of 13.5 kN/m^3; this unit weight was obtained by pouring sand from a height of 240 mm. After the pouring of the soil into the steel container was completed, the surface layer was scraped and leveled to get a flat surface, after which the installation process of the model pile was done to drive the pile into the soil.

The model pile was driven into the soil to the desired depth using a hydraulic jack. Before the driving process, the pile was pushed into the soil bed by hand to an approximate depth of 100 mm. Then, the pile was left standing and the verticality of the pile was checked and adjusted. Special care was given to make sure that the line joining the center of the pair of strain gauges coincided with the centerline of the surcharged area that was used to simulate the embankment. Subsequently, the hydraulic jack was secured to the model pile head and the driving process was started. The hydraulic jack had a maximum length of 400 mm; an extension rod was used to extend the maximum length of the jack. The pile verticality was checked and adjusted during the test when necessary.

3   Testing Procedure and Data Processing

The model pile was loaded up to 200% of the working load and divided into eight increments each equals 25% of the working load. The pile head was located at 140 mm above the sand surface with 360 mm as embedded length. This method of load application put no restriction on the head of the pile; hence the pile was simulated in free head condition. The failure criterion adopted was that proposed by Terzaghi [22], where the failure load corresponds to a displacement of 10% of the footing or pile width/diameter. The following procedure was followed to study the effect of a nearby embankment construction on axially loaded and unloaded model piles:

1. Preparing of the soil bed by using the raining technique.
2. Connecting the channels of the strain gauges pairs to the tested model piles to the data logger.
3. Driving the first model pile (LP-loaded pile) at a distance larger than (10) D from the walls of the steel container to avoid the effect of tip resistance [23]; then drive the second model pile (UP-unloaded pile) at a distance larger than

(15) D to eliminate any rigid boundary [24]. Special attention was given to ensure that the line joining the center of the pair of strain gauges coincided with the centerline of the surcharged area that was used to simulate the embankment.

4. Applying axial load to the model pile (LP) equal to the working load.
5. Installing two mechanical dial gauges for each model pile (LP and UP) that were placed horizontally to measure the horizontal displacement of the model piles at two points along the upper part of the model piles over the soil surface: one of them at the soil surface and the second at a distance from the soil surface.
6. Applying the surcharge load to the steel plate, which was used to simulate the embankment, as shown in Figure 2, with increments of (10, 20, 40, 40, 50, and 60 kPa), where each increment maintained for 2 minutes, i.e. equal to 14.9 days in 1g model [25-27]. Generally, the embankment used in this study was a simulation for the loading of an adjacent building transmitted from a new foundation to an existing foundation. Mostly, the foundation of a construction is considered rigid, but in some cases, such as embankments, the loading is considered flexible [16, 17, 25-28].
7. Recording the dial gauges readings with times was done during each loading increment. Also, the readings of the strain gauges for each load increment were saved in the data logger.
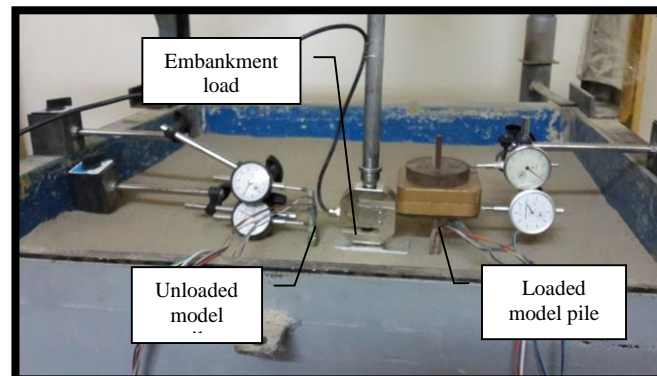

Figure 2 Physical model of loaded and unloaded passive piles.

The strain gauges were fixed in four locations to the model piles to measure the strains generated during the test. Then the bending moment could be calculated from the measured strain in the same locations. The flexural stress (σ_z) was calculated from the measured bending strain (ε_z) by using Hooke's Law (Eq. 1). Then the discrete bending moment (M) was calculated from the flexural stress (σ_z) by applying the elastic flexure formula for beams under bending (Eq. (2)).

$$\sigma(z) = E_p \ \varepsilon(z) \tag{1}$$

$$M(z) = \frac{2 \ \sigma(z) \ I_p}{D} = \frac{2 \ E_p \ I_p}{D} \varepsilon(z) \tag{2}$$

where $\sigma(z)$ is the stress; E_p is the modulus of elasticity of the pile; $\varepsilon(z)$ is the strain; $M(z)$ is the bending moment; I_p is the inertia moment of the model pile section; D is the outer diameter of the model pile. According to the beam theory, four parameters expressing the pile responses (displacement, rotation, shear force, and soil reaction) were derived from the bending moment. The sheer force and the soil reaction can be obtained by differentiating the bending moment profile to the first and the second order respectively. Also, the pile rotation and deflection can be obtained by integrating the bending moment profile to the first and the second order respectively (See Eqs. (3) to (6)).

$$y(z) = \int (\int \frac{M(z)}{E_p \ I_p} \ dz) \ dz \tag{3}$$

$$S(z) = \int \frac{M(z)}{E_p \ I_p} \ dz \tag{4}$$

$$T(z) = \frac{dM(z)}{dz} \tag{5}$$

$$P(z) = \frac{d^2 M(z)}{dz^2} \tag{6}$$

where z is the depth measured from the soil surface; M (z) is the bending moment at depth z; y (z) is the lateral deflection of the model pile; S (z) is the rotation of centerline of the model pile in radians; T (z) is the shear force along the shaft of the model pile; P (z) is the soil reaction along the shaft of the model pile. To obtain the pile response, the bending moments were then subjected to an extensive analysis and data processing. One approach involved fitting the profile to a best-fit polynomial curve, which ranged from the fourth to the seventh order, to obtain the continuous distribution of the bending moment profile along the pile length [25,28-30]. Numerical integration with the trapezoidal rule was used in the current study to integrate the bending moment profile in order to derive the pile rotation and pile deflection profiles. Once the pile rotation profile was obtained, it was further integrated to derive the pile deflection. The integration constants, which consisted of the pile rotation (S_0) and the pile deflection (y_0), at the soil surface, were measured directly from the displacement measured by the dial gauges mounted to the pile head in Eqs. (7) and (8).

$$S_i = \sum_{i=0}^{n} \frac{M_i + M_{i+1}}{2} \Delta z - S_o \tag{7}$$

$$y_i = \sum_{i=0}^{n} \frac{S_i + S_{i+1}}{2} - \Delta z - n \Delta z \ S_o + y_o \tag{8}$$

For the finite difference method to be applied easily to the pile, the strain gauges were spaced at equal lengths (Δz), as shown in Figure 1. The strain measurement, in terms of bending moment, was measured at each point of the pile. The bending moment was plotted against depth (z) at the final increment of the surcharge load. Consequently, the shear force (T_i) could be obtained by differentiating the bending moment (M_i). This differentiation was achieved by using the 1st-order finite differentiation.

$$T_i = \frac{1}{2}\frac{M_{i-1} - M_{i+1}}{\Delta z} \tag{9}$$

The soil reaction can be obtained by the second-order finite differentiation, as noted by Levachev $et\ al.$ [31]. This method offers a more reliable value for the soil reaction and exact results when compared to the common finite difference method.

$$P_i = \frac{1}{7}\frac{2M_{i-2} - M_{i-1} - 2M_i - M_{i+1} + 2M_{i+2}}{\Delta z^2} \tag{10}$$

Eq. (10) requires five measured bending moments to drive the soil reaction (P_i) at a point located on the pile. Thus, P_1, P_2 and P_3 could be derived easily from the five bending moments measured directly on the pile. However, to derive the soil reaction (P_4), the imaginary bending moments, M_5 and M_6, had to be predetermined. With known boundary conditions at the pile tip, M_6 can be calculated with the method described by Scott [32]. The bending moment and shear force at the pile tip were zero, $T_{tip} = 0$ and $M_{tip} = 0$, by substituting the value of shear force at the pile tip into Eq (9), taking $\Delta z = 60$ mm, we obtain $M_5 = M_4$. Similarly, taking $\Delta z = 180$ mm, we have $M_6 = M_3$.

4   Results and Discussion

The results obtained from the vertical loading tests and the tests of the simulated embankment nearby an axially loaded pile are presented and discussed in this section. Two parameters were studied in this section: the axial load applied to the top of the model pile and the distance between the face of the model pile and the edge of the embankment. The load-settlement curve for the model pile is shown in Figure 3. The predicted ultimate carrying capacity of the pile was 50.1 N and the measured value of ultimate carrying capacity obtained from the loading test was 38 N. The effects of the simulated embankment construction adjacent to the pile were studied at three different distances from the edge of the model pile: 2.5, 5, and 10 D (D is the outer diameter of the used pile). The model piles were tested under two different axial load conditions: (1) subjected to axial load equal to its working load, and (2) left without any load on its free head. The results discussed in this section are: head displacement, bending moment profiles, and pile deflection profiles. The rotation profile of the pile showed a small difference

between the head and the tip of the pile. The effect of axial load application did not appear in the model piles because it acts as a relatively rigid pile according to the flexibility factor (K_R), which is defined as follows [21]:

$$K_R = \frac{E_p I_p}{E_s Le^4} < 10^{-5} \tag{11}$$

where E_p is the modulus of elasticity of the pile; I_p is the moment of inertia of the cross-sectional area of the model pile; E_s is the secant modulus of elasticity of the soil; Le is the embedded depth of the model pile.
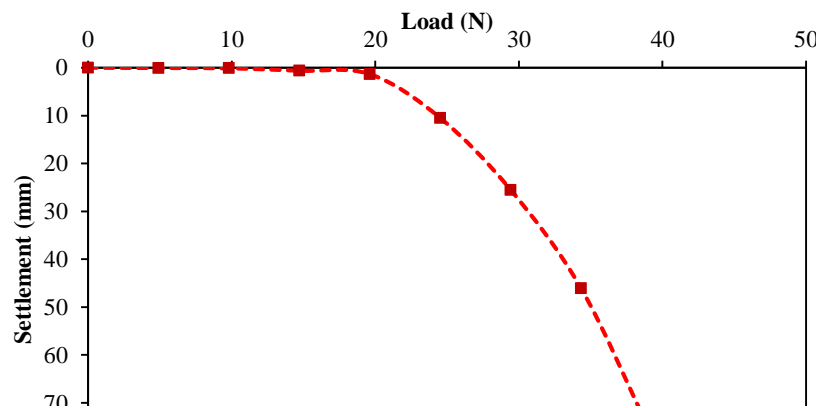
Figure 3 Load-settlement curve of the model pile.

The results of model pile displacement at the soil surface showed a decrease in the maximum displacement by (58-64) % and (31-50) % for LP and the UP, respectively, as shown in Figure 4. This range of decrease was noticed by increasing the spacing between the pile and the constructed embankment from 2.5 to 10 D. The embankment applies a vertical load to the surface of the soil, which causes densification of the soil under the embankment and soil to move away from the source of loading due to the weak structure of the sandy soil used in this work.

The movement of the soil will apply pressure on the front side (near from embankment) of the pile and the value of such pressure decreases with increasing spacing between the face of the pile and the edge of the embankment. The displacement of the rigid unloaded pile was more than the displacement of the flexible pile by 45%, 32%, and 11% at 2.5, 5, and 10 D, respectively. The application of axial load to the head of the pile restrained the rigid pile more than the flexible pile, where the displacement of the loaded rigid pile was less than that of the loaded flexible pile by 6% and 42% at distances 5 and 10 D respectively [33].
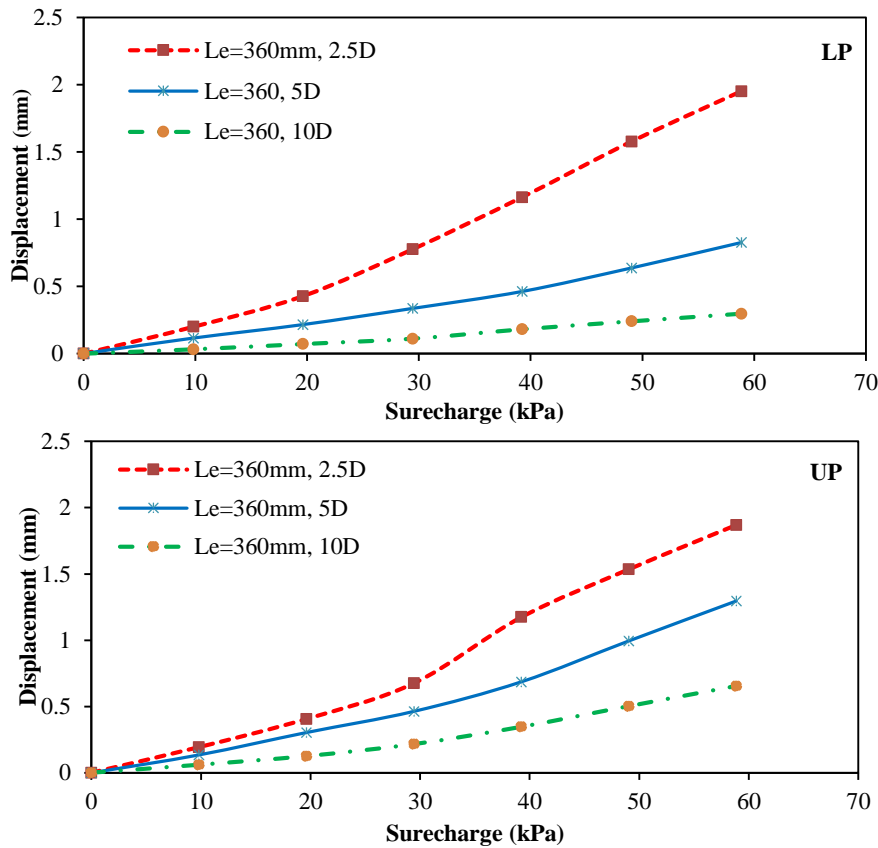
Figure 4 Displacement of the piles at the soil surface.

The rotations at the soil surface of LP and UP at different distances between the embankment and the edge of the pile are shown in Figure 5. The rotation at the soil surface of LP decreased by (64-75) % by increasing the distance between the embankment and the edge of the pile from 2.5 to 10 D. This reduction in rotation resulted from the rigidity of the pile and the application of axial load.

The rotation at the soil surface of UP was decreased by (28-59) % by increasing the distance from 5 to 10 D because the pile was not restrained by axial load, where the pile moved toward the embankment. The maximum rotation of the rigid pile was more than that of the flexible pile by 156% at 2.5 D, while the maximum rotation at the soil surface of the rigid pile was less than that of the flexible pile by 28% and 88% at 5 and 10 D, respectively [33].
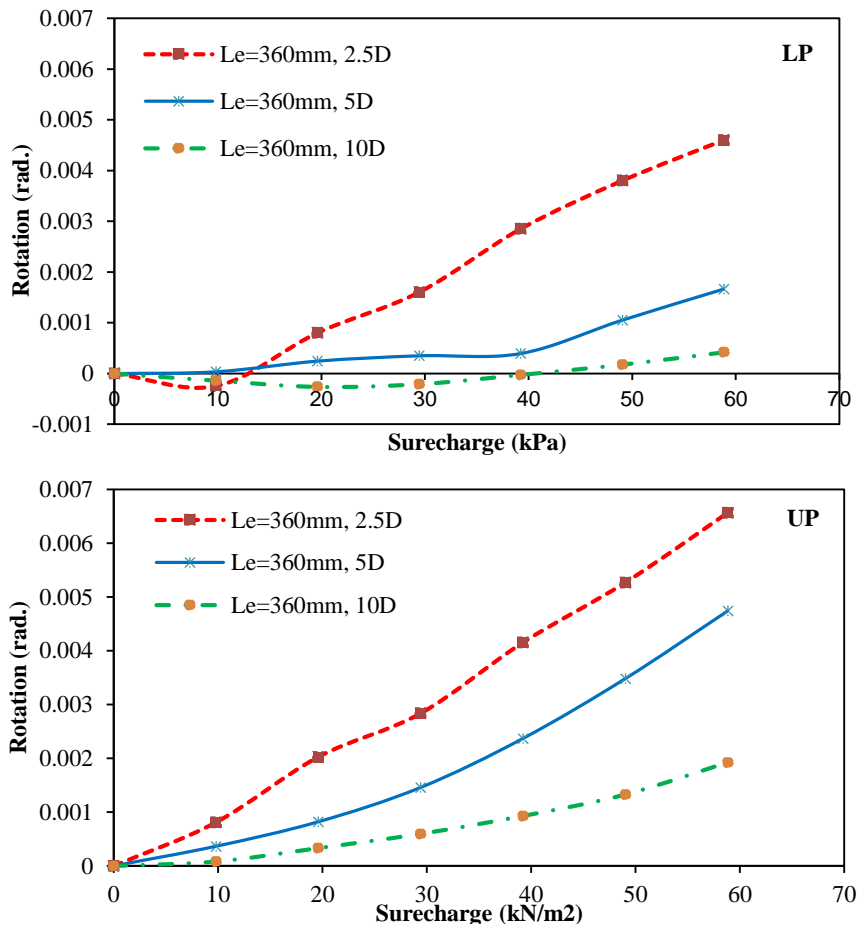
Figure 5 Rotation of the piles at the soil surface.

The bending moment profiles of LP are shown in Figure 6. The total embedded length of the pile underwent soil movement pressure, which means that the flexible pile provided more resistance to the soil movement pressure at distance 2.5 D than the rigid pile. The percentage of the pile length subjected to soil reaction of the total embedded length increased with increasing distance, reaching 86% for the flexible pile and 71% for the rigid pile due to the reduction in soil movement, which was limited at a shallow depth of 5 D. At distance 10 D, the percentage kept increasing up to 83% for the rigid pile, while the percentage decreased to 71% for the flexible pile. The unloaded pile, UP, showed the same behavior as the loaded pile, but the percentages increased more than that of the loaded pile because the pile was not restrained with axial load application. The maximum moment caused by the soil reaction exerted on the pile was increased

by 33% and 200% for LP and UP, respectively. The bending moment profiles are shown in Figure 6, where the maximum bending moment begins with a positive sign when the distance was equal to 2.5 D, which means that the pile bent because of soil movement pressure. When the distance increased from 2.5 D to 5 D, the moment of the soil movement that acted on LP was reduced by 175% and 25% for LP and UP respectively.
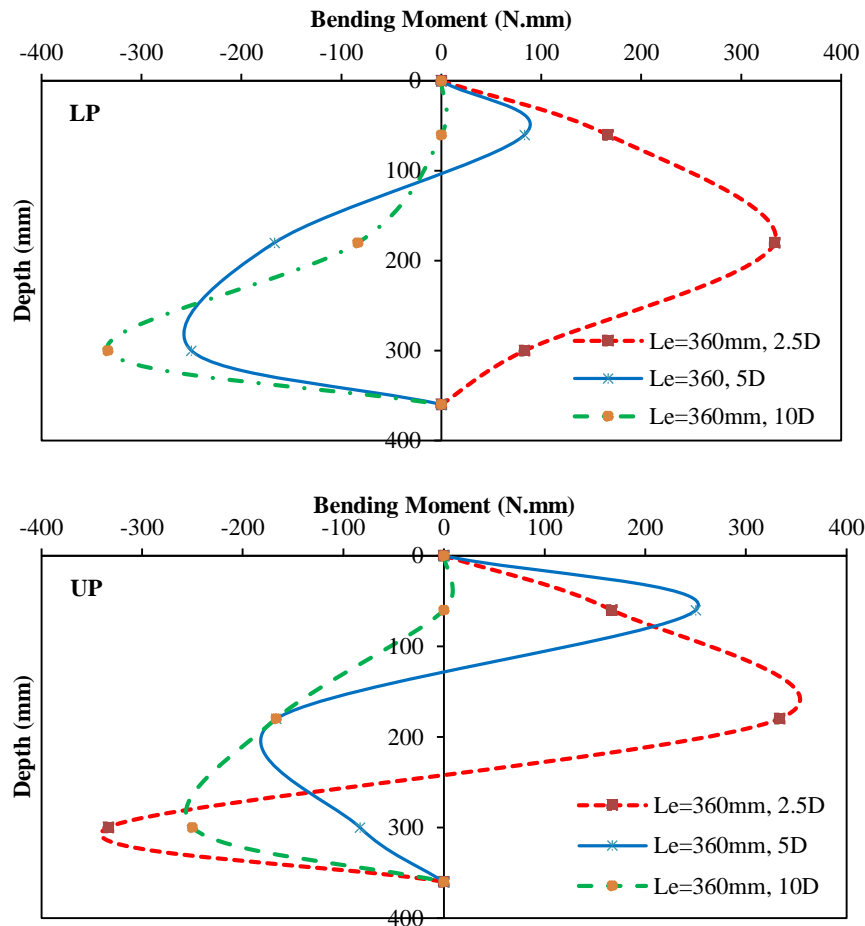

Figure 6 Bending moment profiles of the piles.

The deflection profiles of the axially loaded piles are shown in Figure 7. The maximum deflection decreased by (59-66) % in LP and by (33-142) % in UP when the distance was increased from 2.5 to 10 D. The maximum deflection of LP was located at the pile head due to the application of axial load, which restrained the tip when the embankment was at 2.5, 5, and 10 D, while it was

located at UP tip for 2.5 and 5 D and at UP head for 10 D. The deflection profiles of LP were crossed at one point at a depth of 180 mm from the soil surface and a distance of 0.2 mm from the original location of the pile. This means that the piles were moved by the soil movement over 0.2 mm due to the weak structure of the sand medium and then rotated away from the loading source. Meanwhile for UP, the point of crossing was at a shallow depth, equal to 110 mm, and a distance of 0.3 mm from the original pile location because the piles were not loaded with any axial load.
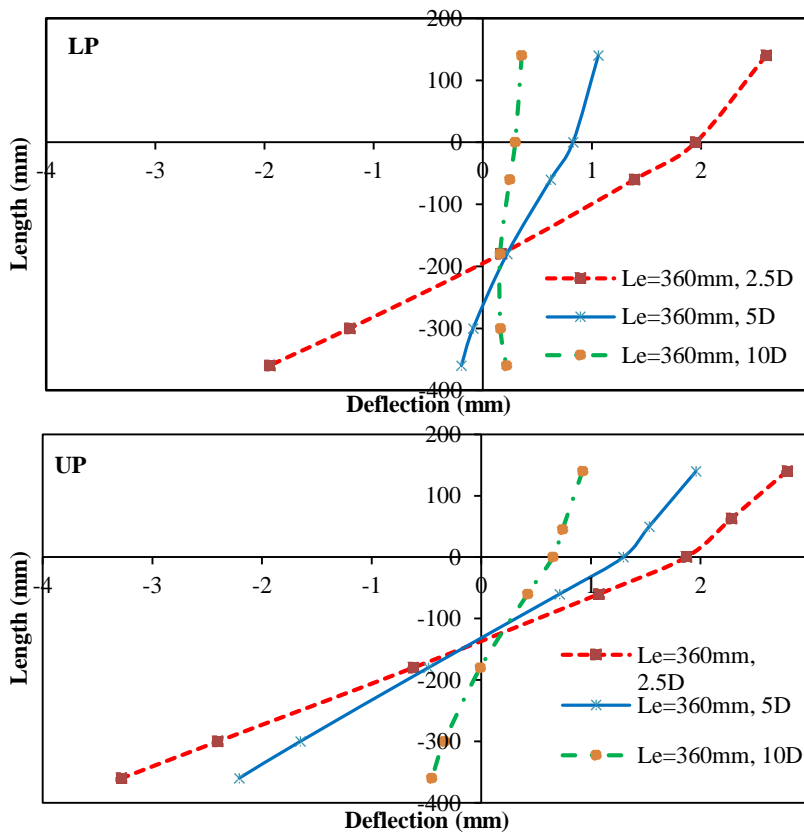

Figure 7 Deflection profiles of the piles.

The rotation profiles show that the maximum rotation of the rigid LP was larger than that of the flexible LP by 177% at distance 2.5 D due to the increase in soil movement pressure, which caused more rotation in the rigid pile, while at 5 and 10 D the rotation of the flexible LP was larger than that of the rigid LP by 22% and 140% respectively due to the pile's flexibility and application of axial load [33]. The maximum rotation of the rigid UP was larger than that of the flexible

UP by 725% and 52% at distances 2.5 D and 5 D respectively, while at 10 D the reverse was noticed. The maximum rotation of the pile decreased by (77-187) % in LP and decreased by (35-64) % in UP by increasing the distance from 2.5 to 10 D due to the rigidity of the piles, as shown in Figure 8.
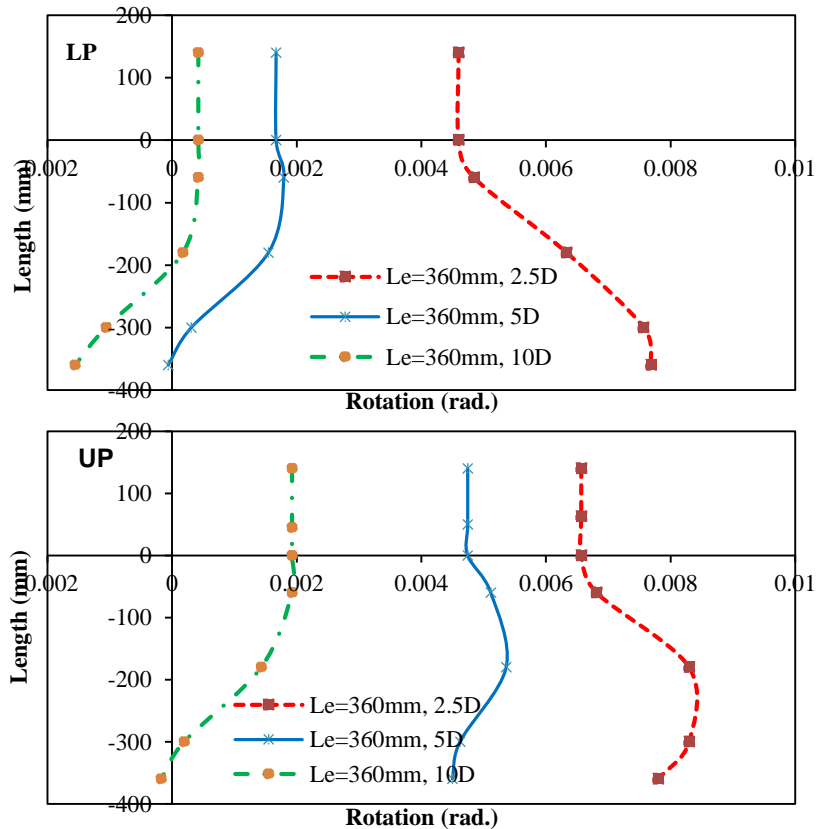

Figure 8 Rotation profiles of the piles.

The maximum shear force of the flexible LP was increased by 175%, 50%, and 33% compared to that of the rigid LP at distances 2.5, 5, and 10 D respectively. Also, the maximum shear force in the flexible UP was larger than that in the rigid UP by 200% and 25% at distances 5 and 10 D for the same reason, while at 2.5 D, the flexible UP moved through the soil due to the high soil movement pressure, which caused a reduction in shear force by 33% compared to that for the rigid UP [33]. The shear force depends on the reduction of the maximum bending moment with increasing distance between the model pile and the embankment, because this reduction comes from the decrease in resistance of the soil behind the pile

due to soil movement, which means that the pile is subjected to more soil movement pressure. The bending moment decreased by 175% and 25% in LP and UP when increasing the distance from 2.5 to 5 D, so the maximum shear force increased by 167% and 175% respectively. When the maximum bending moment increased 33% for the LP, the maximum shear force was not affected, while the decrease of the maximum bending moment by 200% caused a reduction of the maximum shear force to 150% in UP when increasing the distance from 5 to 10 D, as shown Figure 9.
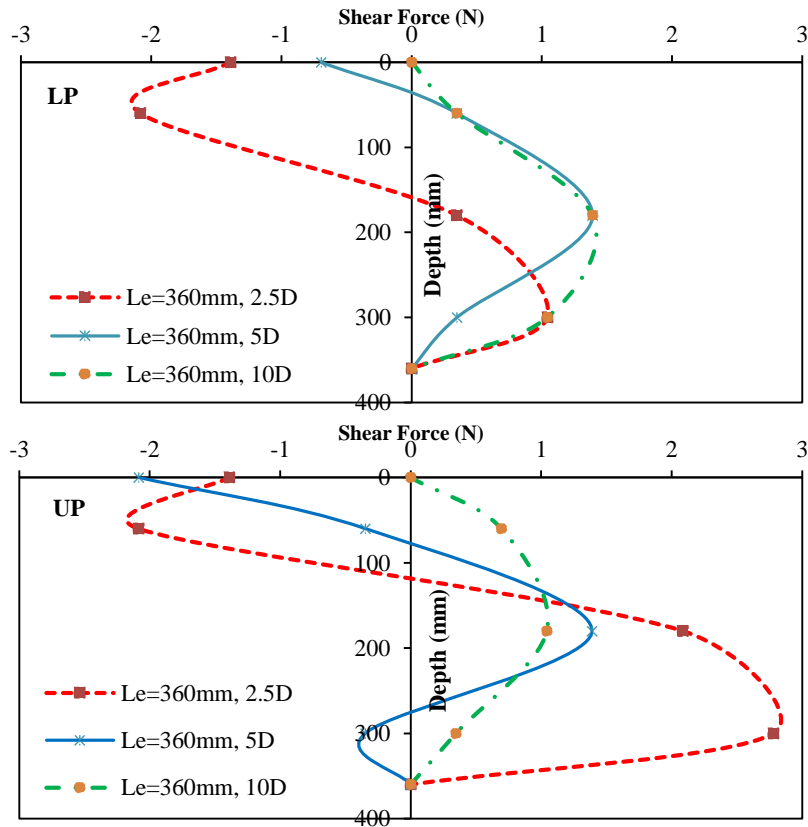

Figure 9 Shear force profiles of the piles.

In the soil reaction profiles, the maximum soil reaction with a negative sign is defined as soil movement, while the soil reaction with a positive sign is defined as soil resistance. Rigid piles with a short-embedded length are subject to soil movement more than flexible piles [33]. The increase in soil movement of the rigid piles in comparison to that of the flexible piles was 88%, 25%, and 0% for LP and increased by 329%, 110%, and 20% for UP at distances 2.5, 5, and 10 D,

respectively, as shown in Figure 10. The soil reaction decreased by increasing the distance between the edge of the pile and the embankment due to the reduction of the soil movement pressure. The maximum soil reaction remained constant for LP due to the rigidity of the pile and application of the axial load which restrained the pile, while it increased to 12% and then decreased to 81% for UP by increasing the distance from 2.5 to 5 D and from 5 to 10 D.
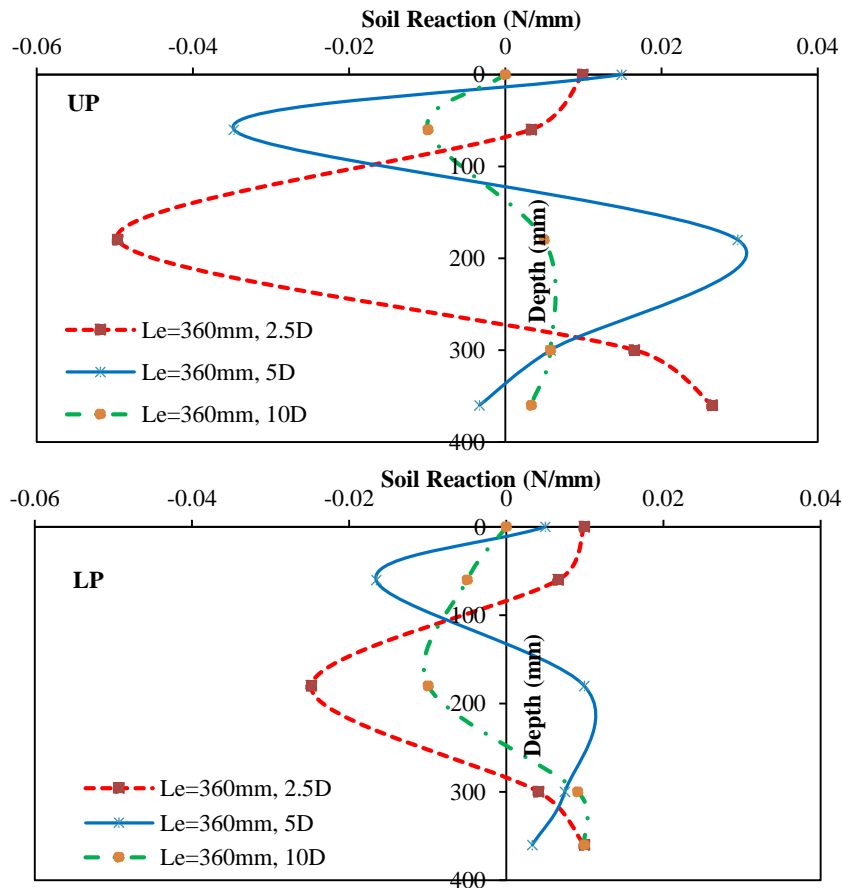

Figure 10 Soil reaction profiles of the piles.

5   Conclusions

The construction of a nearby embankment or surcharge load will affect the behavior of adjacent foundations, especially deep foundations. Based on the results obtained from the present study, the following conclusions can be drawn:

1. The application of an axial load decreased the lateral displacement at the soil surface, where UP was displaced more than LP by 57% and 120% at 5 and 10 D respectively. At 2.5 D, LP was displaced more than UP by 4%.
2. The bending moment of the pile was not influenced by the application of axial loading on the pile due to the high soil movement, where the maximum bending moment of LP and UP at distances 2.5 and 5 D was the same, while at 10 D, the maximum moment for LP was more than for UP by 33%.
3. The maximum deflection of LP was higher than that of UP by 26%, 108%, and 159% at embankment distance 2.5, 5, and 10 D respectively.
4. The shear force depends on the reaction of the soil, so the shear force increases with an increasing reaction of the soil. The maximum soil reaction and shear force for UP was more than that for LP when the embankment was at 2.5 and 5 D respectively, while at 10 D, the maximum soil reaction and shear force for LP was higher than that for UP.
5. The maximum displacement at the soil surface decreased by (58-64) % in LP and (31-50) % in UP by increasing distance between the constructed embankment and the face of the pile from 2.5 to 10 D.
6. The application of axial load increased the soil reaction in flexible piles with a long-embedded length, providing more resistance to soil movement pressure, while a short-embedded length in rigid piles subjected it to soil movement more than that in the case of flexible piles. Also, the soil reaction decreased by increasing the spacing between the existing piles and the embankment.

References

[1]   Salgado, R., Basu, D. & Prezzi, M., *Analysis of Laterally Loaded Piles in Multilayered Soil Deposits*, Joint Transportation Research Program, **330**, 2008.
[2]   Fleming, W.G.K., *A New Method for Single Pile Settlement for Prediction and analysis*, Geotechnique, **42**(3), pp. 411-425, 1992.
[3]   Ercan, A., *Behaviour of Pile Groups under Lateral Loads*, M.Sc. Thesis, Civil Engineering Department, Middle East Technical University, 2010.
[4]   Fleming, W.G.K., Weltman, A.J., Randolph, M.F. & Elson, W.K*., Piling Engineering*, Taylor and Francis, London and New York, 2008.
[5]   Beer, D., *Piles Subjected to Static Lateral Loads*, State of the Art Report, Proc. 9th ICSMFE, 10 Specialty Session, Tokyo, 1–14, 1977.
[6]   Qin, H., *Response of Pile Foundations Due to Lateral Force and Soil Movements*, PhD thesis, Griffith University, School of Engineering, 2010.
[7]   Huat, B.K., Noorzaei, J. & Jaafar, M.S., *Modeling of Passive Piles -An Overview,* Electronic Journal of Geotechnical Engineering, **14**, pp. 1-22, 2009.

[8]   Kahyaoglu, M.R., Imancli, G., Onal, O. & Kayalat, A.S., *Numerical Analyses of Piles Subjected To Lateral Soil Movements*, KSCE Journal of Civil Engineering, **16**(4), pp. 562-568, 2012.

[9]   Zhao, M., Liu, D., Zhang, L. & Jiang, C., *3D Finite Element Analysis on Pile-Soil Interaction of Passive Pile Group*, J. Cent. South Univ. Technol., **15**, pp. 75-80, 2008.

[10]   Yuan, B., Chen, R., Teng, J., Peng, T. & Feng, Z., *Effect of Passive Pile on 3D Ground Deformation and on Active Pile Response*, The Scientific World Journal, **2014**, 904186, 2014. DOI: 10.1155/2014/ 904186.

[11]   Zhang, C.R., Huang, M.S. & Liang, F.Y., *Lateral Responses of Piles Due to Excavation-Induced Soil Movements*, Geotechnical Aspects of Underground Construction in Soft Ground – Ng, Huang & Liu (eds) Taylor & Francis Group, London, 2009.

[12]   Ti, K.S., Huat, B.B., Noorzaei, J., Jaafar, M.S. & Sew, G.S., *Modeling of Passive Piles – An Overview*, Electronic Journal of Geotechnical Engineering, **14**, pp. 415-426, 2009.

[13]   Karim, M.R., Lo, S.C. & Gnanendran, C.T., *Behaviour of Piles Subjected to Passive Loading Due to Embankment Construction*, Canadian Geotechnical Journal, **51**(3), pp. 303-310, 2013.

[14]   Ersoy, C.O. & Yildirim, S., *Experimental Investigation of Piles Behavior Subjected to Lateral Soil Movement*, Teknik Dergi, **25**(4), pp. 6867-6888, 2014.

[15]   Aljorany, A.N., *Analytical Solution to the Problem of Passive Shaft Resistance Due to Lowering of Groundwater Table*, Journal of GeoEngineering, **12**(3), pp. 119-127, 2017.

[16]   Karkush, M.O. & Kareem, Z.A., *Investigation the Impacts of Fuel Oil Contamination on the Behaviour of Passive Piles Group in Clayey Soils*, European Journal of Environmental and Civil Engineering, pp. 1-17, 2018.

[17]   Karkush, M.O. & Kareem, Z.A., *Behavior of Passive Pile Foundation in Clayey Soil Contaminated with Fuel Oil*, KSCE Journal of Civil Engineering, **23**(1), pp. 110-119, 2019.

[18]   Ren, G.F., Xu, G.M., Gu, X.W., Cai, Z.Y., Shi, B.X. & Chen, A.Z., *Centrifuge Modelling for Lateral Pile-Soil Pressure on Passive Part of Pile Group with Platform*, in Physical Modelling in Geotechnics, **1**, pp. 583-587. CRC Press, 2018.

[19]   American Society for Testing and Materials, *Annual Book of ASTM Standards: Soil and Rock*, ASTM, Philadelphia, PA, 2003.

[20]   British Standards BS 1377, *Methods of Testing for Civil Engineering Purpose*, British Standards Institution, London, 1976.

[21]   Poulos, H.G. & Davies, E.H., *Pile Foundation Analysis and Design*, Wiley, New York, N.Y, 1980.

[22]   Terzaghi, K., *Theoretical Soil Mechanics*, Wiley, New York, 1944.

[23]   Bolton, M.D., Gui, M.W., Garnerier, J., Corte, J.F., Bagge, G., Laue, J. & Renzi, R., *Centrifuge Cone Penetration Tests in Sand*, ASCE, **49**(4), pp. 543-552, 1999.

[24]   Kishida, H., *The Ultimate Bearing Capacity of Pipe Piles in Sand*, Proceedings of the 3rd Asian Regional Conference of Soil Mechanics and Foundation Engineering, **1**, pp. 196-199, 1967.

[25]   Springman, S.M., *Lateral Loading on Piles Due to Simulated Embankment Construction*, Unpublished Doctoral Dissertation, Cambridge University, England, 1989.

[26]   Bransby, M.F., *Piled Foundations Adjacent to Surcharge Loads*, Unpublished Doctoral Dissertation, University of Cambridge, England, 1995.

[27]   Bransby, M.F. & Springman, S.M., *Centrifuge Modeling of Pile Groups Adjacent to Surcharge Loads*, Soils and Foundations, Japanese Geotechnical Society, **37**(2), pp. 39-49, 1997.

[28]   Stewart, D.P., *Lateral Loading of Piled Bridge Abutments Due to Embankment Construction*, Unpublished Doctoral Dissertation, University of Western Australia, Australia, 1992.

[29]   Chen, L.T. & Poulos, H.G., *Piles Subjected to Lateral Soil Movements*, Journal of Geotechnical and Geoenvironmental Engineering, **123**(9), pp. 802-811, 1997.

[30]   Chen, F. & Yang, M., *Numerical Analysis of Piles Influenced by Lateral Soil Movement Due to Surcharge Loads*, Chinese Journal of Geotechnical Engineering, **27**(11), pp. 1286- 1291, 2005.

[31]   Levachev, S.N., Fedorovsky, V.G., Kurillo, S.V. & Kolesnikov, Y.M., *Piles in Hydrotechnical Engineering*, Taylor and Francis, 2002.

[32]   Scott, R.F. *Foundation Analysis*. Prentice-Hall, Englewood Cliffs, NJ, 1981.

[33]   Karkush, M.O., Aljorany, A.N. & Jaffar, G.S., *Behavior of Passive Single Pile in Sandy Soil*, IOP Conf. Series: Materials Science and Engineering, **737**(012106), pp. 1-12, 2020.